approximately constant. Flux density in the stator and rotor cores can be expressed as follows [14]:

$$B_{cs} = \begin{cases} 5.47 f^{-0.35} & f > 40Hz \\ 1.7 \rightarrow 1.8 \ (T) & f \le 40Hz \end{cases} \quad \text{(a-9)}$$

$$B_{cr} = 1.6 \rightarrow 1.8 (T)$$

The calculation of the electromagnetic torque is based on Maxwell's tension method as in the following:

$$T_e = pR_m(R_o - R_i) \cdot \int_0^{\lambda} \frac{\vec{B}_x \cdot \vec{B}_y}{\mu_0} dl \quad \text{(a-10)}$$

The total losses are due to the Ohmic losses of the stator windings, the eddy current in conductors, core losses, and the friction and windage losses. By means of analytic model the losses due to harmonic components can be considered, too. The efficiency is calculated by the following equation:

$$\eta = \frac{T_e \omega_m}{T_e \omega_m + P_{RI^2} + P_e + P_{edd} + P_h} \quad \text{(a-11)}$$

8. REFERENCES

[1] J. R. Bumby, R. Martin, M. A. Mueller, E. Spooner, N. L. Brown, and B. J. Chalmers, "Electromagnetic design of axial-flux permanent magnet machines," Proc. Inst. Elect. Eng., Elect. Power App., vol. 151, no 2, pp. 151-160, March 2004.

[2] J. Azzouzi, G. Barakat, and B. Dakyo, "Quasi-3d analytical modelling of the magnetic field of an axial flux permanent magnet synchronous machine," in Proc. IEMDC'2003, Wisconsin, USA, 2003, pp. 1941-1947.

[3] G. U. Qishan, H. Zhong, and Q. Hao, "Three-dimensional field computation for permanent magnet electric machines with finite axial magnet length," Electrical Engineering, Springer-Verlag 2003.

[4] E. P. Furlani and M. A. Knewtson, "A three-dimensional field solution for permanent-magnet axial-field motors," IEEE Trans. Magn., vol. 33, no 3, pp. 2322-2325, May 1997.

[5] M. Mirzayee, and M. Mirsalim, "Use of ferrite in the core of high-speed disk induction motors ", The 9th International Conference on Ferrites, The American Ceramic Society, August 22-27, 2004, San Francisco, U.S.A.

[6] S. E. Abdollahi, M. Mirsalim, M Mirzayee, M. Ehsani, and S. Gay, "Two-dimensional finite element and analytical modelling of a solid rotor disk induction motor", International Scientific Quarterly 'ELECTROMOTION' (ISSN 1223 – 057X), Vol. 10, No. 3, 2003

[7] S. E. Abdollahi, M. Mirsalim, and M. Mirzayee, "Electromagnetic field calculation in an axial flux solid rotor induction machine", The 46th IEEE Midwest Symposium on Circuits and System. MWSCAS, December 27-30, 2003

[8] Dong-Hyeok Cho ; Hyun-Kyo Jung ; Cheol-Gyun Lee, "Induction motor design for electric vehicle using a Niching Genetic Algorithm", IEEE Transactions on Industry Applications, vol. 37 no. 4 pp.994-999, Jul. 2001.

[9] N.Bianchi, S.Bolognani, "Brushless DC motor design: an optimization procedure using genetic algorithms", IEE-EMD'97, Cambridge (UK), 1-3 September 1997.

[10] Dong-Hyeok Cho ; Hyun-Kyo Jung, "Optimal core shape design for cogging torque reduction of brushless DC motor using genetic algorithm ", IEEE Transactions on Magnetic, vol. 36 no. 4 July pp.1927-1931, Jul. 2000

[11] L-Y. Hsu, M-C. Tsai and C-C. Huang: "Efficiency optimization of brushless permanent magnet motors using penalty genetic algorithms", IEEE, 2003

[12] Kosaka, T. Pollock, C. Shikayama, T. Nakagami, T. Kano, Y. Matsui, N. "Electromagnetic design of switched reluctance servomotor drives GA-based computer aided autonomous", Industry Applications Conference, 2004. 39th IAS Annual Meeting. Conference Record of the 2004 IEEE

[13] P. Campbell, D. J. Rosenberg, and D. P. Stanton, "The computer design and optimization of axial-field permanent magnet motors," IEEE Trans. Power App. System., vol. PAS-100, no. 4, pp. 1490-1497, April 1981.

[14] S. Huang, J. Luo, F. Leonardi, and T. A. Lipo, "A comparison of power density for axial flux machines based on general purpose sizing equations," IEEE Trans. Energy Conversion., vol. 14, no 2, pp.185-192, June 1999.

[15] M. Aydin, S. Huang, and T. A. Lipo, "Design and 3-D electromagnetic field analysis of non-slotted and slotted TORUS type axial flux surface mounted permanent magnet disc machines," International Electrical Machines and Drives Conference, Boston, 2001, pp. 645-651.

In the calculations of efficiency and torque, the harmonic components of the field are also considered to the 31st order. By comparison of the second with the third column in Table 2, one can deduce that:

The number of turns of the winding in the optimum design is less than the primitive design

The volume of the machine has decreased in the optimal design

Also, one can easily Figure out that the copper losses are more than the iron losses in this machine, so to achieve maximum efficiency the number of turns of the winding should be reduced.

TABLE 2
RESULTS OF THE DESIGN OPTIMIZATION

Specifications	Primitive design	(OF) is the efficiency	(OF) is the efficiency and torque-to-volume ratio
Inner to outer diameter ratio	0.58	0.5125	0.58
Pole-arc to pole-pitch ratio	0.85	0.8906	0.8291
Inner diameter of stator core (mm)	140	174.2	120.5
Outer diameter of stator core (mm)	242	339.9	241
Axial length of stator core (mm)	22	31.1	20.5
Axial length of rotor core (mm)	13	17.2	12.1
Axial length of magnets (mm)	7.4	2.9	6.8
Total axial length of machine (mm)	85	79.9	80.8
Number of turns per phase	554	243	510
Efficiency (%)	84.7	88.14	85.42
Torque (Nm)	25.44	25.81	25.67
Volume (m^3)	0.0043	0.0074	0.004

6. CONCLUSION

An improved analytic model of an axial-flux machine was presented in this paper and it was demonstrated that by the consideration of the current being distributed in the whole cross section area of the winding, more accuracy in the prediction of the field could be obtained. The effects of the armature reaction and the harmonics of the field were also considered. The simulation results of the magnetic field by the analytic model were compared with the 2-D finite element analysis. It was observed that the proposed analytic model predicted the magnetic field very accurately within 5% of the finite element method.

7. APPENDIX

The outer diameter of the stator consists of the outer diameter of the stator core and the radial thickness of the winding as it is shown in Figure a.1, i.e.:

$$D_t = D_o + 2W_{cuo} \tag{a-1}$$

Using the space factor of the winding, the outer thickness of the winding can be expressed as in the following:

$$W_{cuo} = \frac{\sqrt{D_o^2 + \frac{2D_g a_s'}{k_{cu} J_s}} - D_o}{2} \tag{a-2}$$

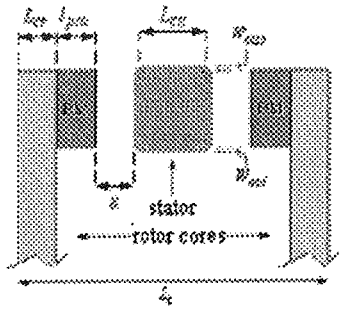

Figure a.1: Front view of an axial-flux permanent magnet machine with two rotor discs and one slot-less stator disc.

In the same way:

$$W_{cui} = \frac{D_i - \sqrt{D_i^2 - \frac{2D_g a_s'}{k_{cu} J_s}}}{2} \tag{a-3}$$

The axial length of the machine is:

$$L_e = L_s + 2L_r + 2g \tag{a-4}$$

According to construction experiences, the following equation is assumed for L_s [14-15]:

$$L_s = L_{cs} + (1.6 \to 2)W_{cui} \tag{a-5}$$

The axial length of the stator core can be obtained by the flux density in the stator core as follows:

$$L_{cs} = \frac{\overline{B}\pi D_o(1+\lambda_d)}{2pB_{cs}} \tag{a-6}$$

The axial length of the rotor core is:

$$L_{cr} = \frac{B_g \pi D_o(1+\lambda_d)}{4pB_{cr}} \tag{a-7}$$

So the axial length of the rotor will be:

$$L_r = L_{cr} + l_{pm} \tag{a-8}$$

where, l_{pm} is the axial length of the magnets, which is calculated in order to have maximum $B_m H_m$ and minimum volume.

The flux magnitude in the stator core is dependent on the converter frequency, but in the rotor core it is

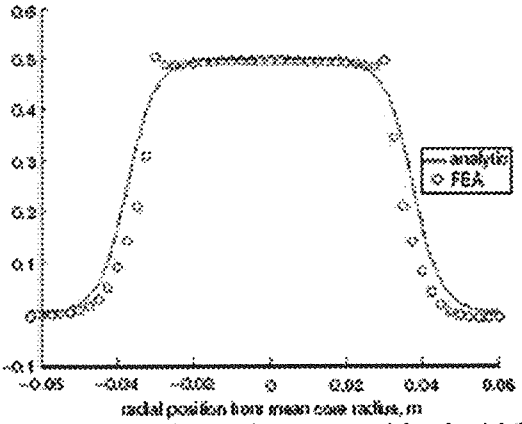

Figure 9: The variation of vector potential and axial flux density with radius [1].

4. Optimal Design

The genetic algorithm (GA), one of the global optimization methods, is well known as a fine method to optimize the design of electrical machines [8-12]. Here, the authors implemented GA to optimally design an axial-flux machine.

A. The Problem Formulation

This section presents the approach to determine the optimum dimensions of the machine. The objective function (OF) can be considered as minimum material cost, minimum weight, an optimum performance feature of the motor such as maximum efficiency, torque-to-current ratio, or some other motor Figures or a combination of them. In this paper, two objective functions are implemented; to maximize efficiency, and to reach the best efficiency and torque-to-volume ratio together as it is desired in most hybrid vehicle applications. The analytic model is utilized to calculate the objective functions. Here, the design variables are the ratio of the inner to outer diameter of the stator core, the ratio of pole-arc to pole-pitch, and the outer diameter of the stator. Due to applications of the machine and some other reasons which will be explained shortly, some constraints on design variables must be considered. Cambel *et al.* [13] have shown that the ratio of pole-arc to pole-pitch, α, should be between 0.75 and 1 to achieve minimum copper losses. So one constraint is taken as $0.75 \le \alpha \le 0.9$, and the upper bound is considered as 0.9 to avoid the flux leakage between two neighbouring magnets. Because of construction problems λ_d cannot be 0 or 1, so the other constraint is taken as $0.1 \le \lambda_d \le 0.9$. Some constraints also arise due to the specific applications. For example, in automotive cases, the following constraint should be considered because of the wheel dimensions:

$$D_i \ge 0.08m \quad , \quad D_o \le 0.35m$$

A sample of calculations for dimensions, torque and efficiency are given in the appendix.

B. Genetic Algorithms

In order to use the GA, the foreseen ranges of the design variables are represented by a binary string. The string length is 30 bits for 3 design variables. So 10 bits are assigned to each variable and the accuracy (quantization) of each variable is $1/2^{10}$. Figure 10 shows a typical chromosome.

X_{1bin}	X_{2bin}	X_{3bin}
0010110100	1110100101	0101001110

Figure 10: A typical chromosome.

The population size consists of 30 individuals (chromosomes) and the probability of crossover and mutation are 0.8 and 0.05, respectively. Another operator which is used is the "immigrant" with a probability of 0.05. One can expand chromosomes and also consider the other independent variables such as the specific electrical and magnetic loadings as design variables.

To accelerate the search procedure, the decoding of substrings are characterised as follows:

$$\lambda_d = 0.1 + 0.8 \times \frac{decimal(X_{1bin})}{1024} \tag{15}$$

$$\alpha = 0.75 + 0.15 \times \frac{decimal(X_{3bin})}{1024} \tag{16}$$

$$D_o = 0.0889 + 0.27 \times \frac{decimal(X_{2bin})}{1024} \tag{17}$$

In this way, a constrained problem is transferred to an unconstrained one.

5. Optimum Results

If one applies the optimization algorithm to a primary design with the data given in the second column of Table 2, the results summarized in the third and fourth columns of the table are obtained.

In this paper as it has been mentioned before, the objective function is once to maximize the efficiency and in another time to reach the best efficiency and torque-to-volume ratio together, as described by the following equation:

$$Objective\ Function = 0.9 * efficiency + 0.1 * \frac{normalized\ torque}{normalized\ volume} \tag{18}$$

It is worth noting that the efficiency is expressed by a normalized number less than 100%, so in (18) the torque and volume ought to be normalized. Now, the weighting factor of each part of the above formula can be changed according to its priority.

3. The Results of The Modelling

A. Analytic Model

The parameters which are used in the analysis are summarized in Table 1[1]. Figure 5 shows the air-gap magnetic flux density for no-load and full-load conditions. One can deduce from this Figure that the armature reaction changes the field in x-coordinate direction, but its effect is small.

TABLE 1
MACHINE PARAMETERS [1]

Number of poles per disc	16	Magnet width in mean radius	41 mm
Turns per armature coil	4	Pole pitch	62 mm
Magnet material	Nd-Fe B	Thickness of winding	3 mm
B_{rem}	1.2 T	Length of Air-gap	5 mm
μ_{rec}	1.05	Thickness of rotor yoke	10 mm
Output power	40 kW	Stator yoke thickness	28.4 mm
Magnet thickness	6 mm	Mean diameter	316 mm

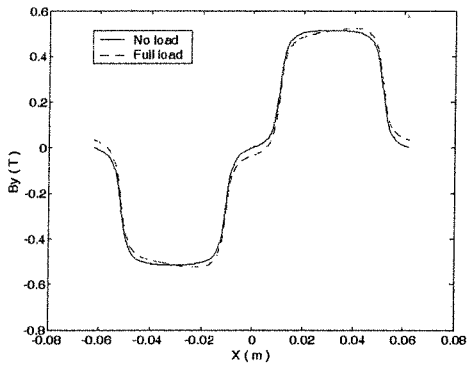

Figure 5: Magnetic flux density for no-load and full-load conditions in region 2 using analytic method.

The magnets are mounted on the rotor and the machine has natural ventilation, so one can use relatively high current densities. Here, the current density is assumed $6.5 A/mm^2$ and also, $x_o = \lambda/2$.

B. FEM

The magnetic flux lines and the flux density distribution for no-load condition are depicted in Figures 6 and 7, respectively.

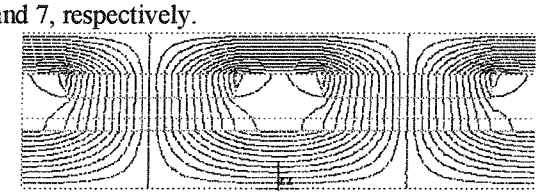

Figure 6: The magnetic flux lines for the no-load condition (FEM).

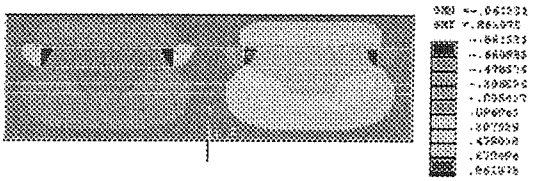

Figure 7: The flux density distribution for the no-load condition (FEM).

The magnetic flux density (at no load) in regions 2 and 3 are compared with each other and also with FEM in Figure 8. The results demonstrate excellent agreement between the proposed analytic and the finite element methods with a maximum discrepancy of less than 5%.

Figures 9 (a) and (b) which show the plot of the variation of vector potential and axial flux density in the radial direction across the surface of the iron stator core for the 40 kW generator, have been taken from [1]. The flux density plots have been obtained using the analytic expressions and 2-D and 3-D finite element analysis (FEA), whereas the analytic and 2-D FEA have been used for the vector potential.

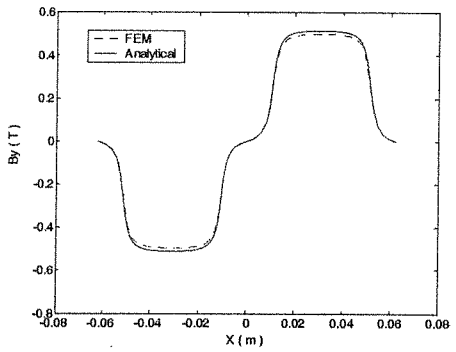

(a)

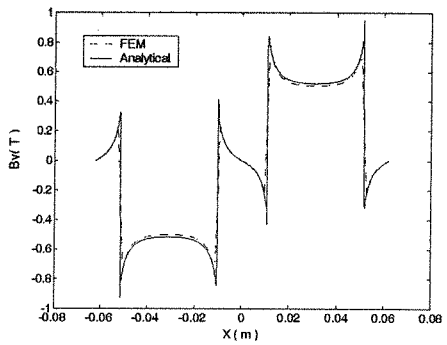

(b)

Figure 8: The magnetic flux density computed with analytic and finite element methods in: a) region 2, b) region 3.

By the comparison of Figure 8 with Figure 9, one can deduce that the magnetic flux density computed with the proposed analytic method resembles the results presented in [1]. As it was written before, the proposed approach is also more accurate.

$$M(x)=\sum_{n=1,3,5,\ldots} -M_n \; Cos\left(\frac{n\pi}{\lambda}(x+x_o)\right)$$

$$M_n=\frac{M}{n}\left(\frac{4}{\pi}\right)Sin\left(\frac{n\pi\, l_m}{2\lambda}\right) \qquad (1)$$

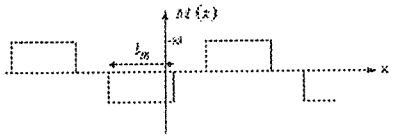

Figure 3: Magnetization distribution of the magnet array.

B. Armature Windings

The three-phase stator windings are shown in Figures 2 and 4. Supposing that j_0 is the surface current density in each phase, the current density distribution in armature windings can be written as in the following:

$$J(x)=\sum_{n=1,3,5,\ldots} J_n \, Sin\left(\frac{n\pi}{\lambda}x\right)$$

$$J_n=\frac{2j_o}{n\pi}\left[\frac{1}{2}Cos\left(\frac{n\pi}{3}\right)-\frac{1}{2}Cos\left(\frac{2n\pi}{3}\right)+1\right] \qquad (2)$$

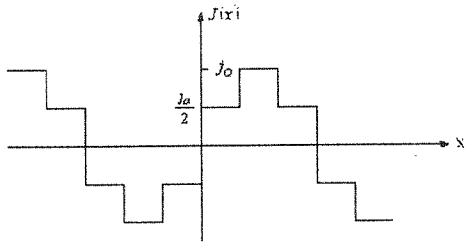

Figure 4: Current density distribution in the armature windings.

This equation is a new form to represent the current density distribution of armature windings, which has been implemented in the analytical modelling for the first time by the authors.

C. Magnetic Field

The governing equations of the magnetic field are given by the following Maxwell's equations:

$$\nabla\times\vec{H}=\vec{J} \qquad (3)$$

$$\nabla\cdot\vec{B}=0 \qquad (4)$$

The magnetization vector of permanent magnets is considered to be constant and thus, $\nabla\cdot\vec{M}=0$ and $\nabla\times\vec{M}=0$. If one recalls that $\nabla\cdot\vec{A}=0$, the Laplace and Poisson equations can be derived from (3) and (4) as in the following in regions 1, 2 and3:

$$\nabla^2\varphi_m=0 \qquad \text{regions 2, 3} \qquad (5)$$

$$\nabla^2\vec{A}=-\mu_o\,\vec{J} \qquad \text{region 1} \qquad (6)$$

where, regions 1, 2, and 3 are the stator winding, the air-gap, and the magnets, respectively.

Solving the Laplace and Poisson equations, the flux density can be expressed in each region as follows:

$$\vec{B}=\nabla\times\vec{A} \qquad \text{region 1} \qquad (7)$$

$$\vec{B}=-\mu_o\nabla\varphi_m \qquad \text{region 2} \qquad (8)$$

$$\vec{B}=-\mu_o\nabla\varphi_m+\mu_o\vec{M} \qquad \text{region 3} \qquad (9)$$

D. Calculation of Magnetic Field

Assuming infinitely permeable iron cores, the tangential component of magnetic field intensity is negligible. Therefore, the boundary conditions are as in the following:

$$H_{x_1}\Big|_{y=0}=0 \;\Rightarrow\; \frac{1}{\mu_o}\frac{\partial A_1}{\partial y}\Big|_{y=0}=0 \qquad (10\text{-a})$$

$$H_{x3}=-\frac{\partial\varphi_3}{\partial x}\Big|_{y=Y_3}=0 \qquad (10\text{-b})$$

Other boundary conditions are:

$$B_{y_3}\Big|_{y=Y_2}=B_{y_2}\Big|_{y=Y_2} \qquad (11\text{-a})$$

$$H_{x3}\Big|_{y=Y_2}=H_{x2}\Big|_{y=Y_2} \qquad (11\text{-b})$$

$$B_{y_1}\Big|_{y=Y_1}=B_{y_2}\Big|_{y=Y_1} \qquad (11\text{-c})$$

$$H_{x_1}\Big|_{y=Y_1}=H_{x_2}\Big|_{y=Y_1} \qquad (11\text{-d})$$

The following expressions are obtained for vector and scalar magnetic potentials, where the subscript denotes the number of region, and y-coordinate represents the axial direction, respectively.

$$A_1(x,y)=\sum_{n=1,3,5,\ldots}\left(S_{11}e^{\frac{n\pi}{\lambda}y}+S_{12}e^{-\frac{n\pi}{\lambda}y}\right)\sin\left(\frac{n\pi}{\lambda}x\right)$$
$$+\sum_{n=1,3,5,\ldots}\left(C_{11}e^{\frac{n\pi}{\lambda}y}+C_{12}e^{-\frac{n\pi}{\lambda}y}\right)\cos\left(\frac{n\pi}{\lambda}x\right) \qquad (12)$$
$$+\sum_{n=1,3,5,\ldots}\mu_o\left(\frac{\lambda}{n\pi}\right)^2 J_n\sin\left(\frac{n\pi}{\lambda}x\right)$$

$$\varphi_2(x,y)=\sum_{n=1,3,5,\ldots}\left(S_{21}e^{\frac{n\pi}{\lambda}y}+S_{22}e^{-\frac{n\pi}{\lambda}y}\right)\sin\left(\frac{n\pi}{\lambda}x\right)+$$
$$\sum_{n=1,3,5,\ldots}\left(C_{21}e^{\frac{n\pi}{\lambda}y}+C_{22}e^{-\frac{n\pi}{\lambda}y}\right)\cos\left(\frac{n\pi}{\lambda}x\right) \qquad (13)$$

$$\varphi_3(x,y)=\sum_{n-1,3,5,\ldots}\left(S_{31}e^{\frac{n\pi}{\lambda}y}+S_{32}e^{-\frac{n\pi}{\lambda}y}\right)\sin\left(\frac{n\pi}{\lambda}x\right)+$$
$$\sum_{n-1,3,5,\ldots}\left(C_{31}e^{\frac{n\pi}{\lambda}y}+C_{32}e^{-\frac{n\pi}{\lambda}y}\right)\cos\left(\frac{n\pi}{\lambda}x\right) \qquad (14)$$

R_m Mean radius of stator core

R_o Outer radius of stator core

T_e Electromagnetic torque

W_{cui} Winding thickness at inner diameter

W_{cuo} Winding thickness at outer diameter

x_0 Position of a magnet pole with respect to a winding pole

Y_1 Winding thickness at mean radius in analytic model

Y_2 The sum of Y_1 and L_g in analytic model

Y_3 The sum of Y_1 , Y_2 and L_g in analytic model

α Ratio of pole-arc to pole-pitch

η Efficiency

λ Pole-pitch

λ_d Ratio of inner diameter to outer diameter of stator

μ_0 Permeability of free space

μ_{rec} Magnetic recoil permeability

φ_m Scalar potential

φ_{m2} Scalar potential in air gap region

φ_{m3} Scalar potential in magnet region

χ_m Magnetic sensitivity

ω_m Mechanical angular speed

1. Introduction

In general, an axial-flux machine comprises of at least one rotor disc carrying either a slot-less or slotted winding. The stator may be magnetic or non-magnetic depending on the machine topology. Based on these concepts, a large number of axial-flux machine topologies are possible including single-sided, double-sided or multistage design [1]. This paper is focused on the slot-less stator, two-rotor axial-flux permanent magnet machine with North-pole to North-pole (NN) structure.

The axial-flux machines have been modelled by several researchers [1-7]. In one of the latest researches, Bumby *et al.* [1] have represented the armature windings by a current sheet close to the iron surface of stator. Here, in this article, the authors have considered the current to be distributed in the whole cross section area of the winding, which yields more accuracy in modelling.

Looking inwards in the radial direction, the structure of the machine can be seen as in Figure 1.

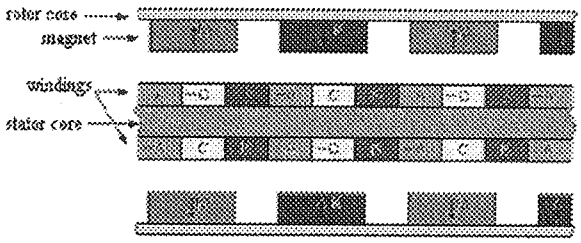

Figure 1: 2-D structure of an axial-flux permanent magnet machine.

The Gramme winding [6] is used around the stator in the air gap between the rotor and stator, and it is assumed that:

- Iron cores are infinitely permeable,
- The magnetization vector of permanent magnets (PM) is constant,
- There is no free space between windings of different phases, and
- With no loss of generality, the space-factor of winding is set to one.

These assumptions will be implemented to obtain the magnetic field equations in the machine. Next, the analytical model is obtained by applying proper boundary conditions and solving these equations in the proposed structure of the machine. Finally, the model is used to design and to calculate the torque and the efficiency of the machine. To achieve more accuracy, the harmonic components of the field are considered too. Based on the accurate model, the machine is designed and is optimized by a Genetic Algorithm (GA) method.

2. The Proposed Analytical Model

A. Modelling of Magnets

Due to the symmetry, the analysis can be done on half of the machine as shown in Figure 2, where the x and y-coordinates represent the circumferential and the axial directions, respectively. The model assumes the radial direction to be infinite.

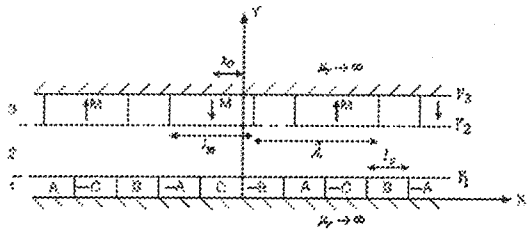

Figure 2: Simplified 2-D structure of an axial-flux permanent magnet disc machine for magnetic field computation.

In modelling axial-flux machines, finite element method can be used. However, this method in an iterative optimization algorithm is time consuming if not difficult. Thus, in this paper an analytical model for axial-flux machines is developed and implemented. As it is shown in Figures 2 and 3, the magnetization distribution of the magnet array may be expressed by Fourier's expansion as follows:

A Modified Analytical Approach in Modelling and Design of Axial-Flux Permanent Magnet Machines

Mohammad Mardaneh[i]; Mojtaba Mirsalim[ii];Mehdi AliAhmadi[iii]

ABSTRACT

In this paper, a modified analytic approach to the calculation of magnetic field in a slot-less, two-rotor axial-flux permanent magnet machine is presented. The analytic-modelling is based on calculation of scalar and vector magnetic potentials which are produced by the armature windings and the magnets. The magnet and the armature windings are modelled by a magnetization vector and a two-dimensional current sheet, respectively. The effects of the armature reaction and the harmonics of field are also considered. The simulation of magnetic field by the analytic model is compared with that of a two-dimensional finite element analysis. The proposed analytic model predicts the magnetic field within 5% compared to the finite element method. Ultimately, by using the analytic model in a genetic algorithm method, which is a known method in optimization, an optimum design of an axial-flux permanent magnet machine is presented.

KEYWORDS

Axial-Flux Permanent Magnet Machine, Analytic Model, Finite Element Method, Genetic Algorithm, Optimum Design.

SYMBOLS

A Vector potential
a_s' Specific electrical loading
a_z Cross section area of wire
B Flux density
$\overline{B}$ Specific magnetic loading
B_{cr} Flux density in rotor core
B_{cs} Flux density in stator core
B_g Flux density in air gap
D_g Mean diameter of stator
D_i Inner diameter of stator core
D_o Outer diameter of stator core
D_t Outer diameter of stator
f Frequency
g Air gap length (magnet to the winding)
H Magnetic field intensity
J_s Current density (A/mm^2)
K_{cu} Copper space factor
L_{cr} Axial length of rotor core
L_{cs} Axial length of stator core
L_e Axial length of machine
L_r Axial length of rotor
L_s Axial length of stator
l_{pm} Axial length of magnets
M Magnetization vector of a magnet
P_e Eddy current losses in conductors
P_{edd} Eddy current losses in cores
P_h Hysteresis losses
P_{RI^2} Copper losses in stator windings
p Number of poles
R_i Inner radius of stator core

---

i A Modified Analytical Approach in Modelling and Design of Axial-Flux Permanent Magnet Machines.

M. Mardaneh is a Ph.D. candidate in the Department of Electrical Engineering at Amirkabir University of Technology, Tehran, Iran (e-mail: m_mardaneh@aut.ac.ir).

ii M. Mirsalim is with the Department of Electrical Engineering at Amirkabir University of Technology, Tehran, Iran (e-mail: mirsalim@aut.ac.ir).

iii M. AliAhmadi graduated in 2005 from the Department of Electrical Engineering at Amirkabir University of Technology, Tehran, Iran (e-mail: m_aliahmadi@yahoo.com).